ARTICLE

Controlling the degradation of cellulose scaffolds with Malaprade oxidation for tissue engineering

Received 00th January 20xx,
Accepted 00th January 20xx

DOI: 10.1039/x0xx00000x

Wichchulada Chimpibul[a,b] , Tadashi Nakaji-Hirabayashi[c], Xida Yuan[b], Kazuaki Matsumura[*b]

This study was conducted to develop biodegradable cellulose scaffolds by oxidising porous cellulose sponges for tissue engineering applications. Cellulose powder was dissolved in ionic liquid using a salt leaching method, and porous cellulose scaffolds of various pore sizes were prepared. The scaffolds were oxidised with periodate to introduce aldehyde at a rate controlled by the periodate concentration. Oxidised scaffolds exhibited weight loss in cell culture medium, but not in phosphate buffer. Therefore, we confirmed that Schiff base formation between the aldehyde and amino groups through a Maillard reaction triggered cellulose molecular degradation. The degradation rate was controlled by the oxidation degree, whereas the aldehyde content controlled protein adsorption and cell proliferation. Additionally, *in vivo* implantation tests revealed that optimising the oxidation ratio not only improved biodegradability but also reduced inflammation. In conclusion, our results suggest that simple oxidised cellulose is useful as a low-toxicity biodegradable scaffold.

INTRODUCTION

The pinnacle of tissue engineering is regenerating a patient's own tissues and organs by using medical technology to promote self-healing[1]. Three important tissue engineering tools are stem cells, scaffolds, and biological signal molecules such as growth factors[2]. The biomaterials in scaffolds play an important role in many cellular activities, such as cell attachment and migration, delivery and retention of cells, and diffusion of vital cell nutrients[3]. Scaffolds not only play a role in cell growth, but also serve as receptor sites for biological and physical stimuli that promote the regeneration of surrounding tissues[4]. Scaffold materials must have specific properties such as high levels of pore interconnectivity, porosity, biocompatibility, and biodegradability[5]. Over the past several decades, researchers have focused on developing scaffold materials from biodegradable polymers such as aliphatic polyesters[6,7] of polylactic acid and polycaprolactone or from naturally derived polymers of proteins, polypeptides,[8] and polysaccharides[9]. Synthetic biodegradable polymers can be easily designed but tend to have low biocompatibility. In contrast, naturally derived polymers have low toxicity and can be easily chemically modified, but they are difficult to purify, and their properties fluctuate across different batches.

Of the natural polysaccharide biopolymers, cellulose is the most abundant, and can be processed into a variety of forms[5,10,11]. Recently, cellulose nanofibers have been studied as next-generation biomedical materials because of their eco-efficiency, environmental degradability, and reinforcing effects when incorporated into various plastics[12–14]. Because of its linear and regular structure and hydroxyl groups, cellulose can form ordered crystalline structure. As a result, it is difficult for cellulose to dissolve in physiological conditions. Additionally, cellulose cannot be degraded in the human body owing to the lack of cellulase. This is one of the limitations of using cellulose as a biomaterial, as the long-term presence of foreign materials in the body can induce inflammation.

Researchers have attempted to overcome this limitation by chemically modifying cellulose to decrease its crystallinity and increase its biodegradability[15,16]. Chemically modifying cellulose by oxidation enhances the specific properties of different cellulose types, leads to the generation of products with added value, and modulates the chemical behaviour of cellulose and its macroscopic properties[15]. The introduction of carboxyl groups using nitric dioxide was reported in 1942[17], and oxidised cellulose containing carboxyl groups has many beneficial medical applications[18]. For instance, 2,2,6,6,-tetramethylpiperidine-1-oxyl-mediated oxidation is used to create cellulose nanofibers[19]. This process enables the development of uniform hydrogels for soft tissue scaffolds and drug delivery carriers. The Malaprade oxidation reaction is another popular and facile oxidation process that oxidises 1,2-diols into dialdehydes or diketones[20]. As polysaccharides have many 1,2-diol moieties, this reaction is frequently used for many applications, including the production of oxygen-barrier coating materials for cellulose[21]. Periodate oxidation of cellulose results in the formation of two aldehyde groups per glucose unit[22], forming 2,3-dialdehyde cellulose. These aldehydes can be utilised to further modify cell adhesion moeities[23].

In our previous study[24–28], we prepared aldehyde-containing dextran using the Malaprade oxidation reaction. Dextran is one of the most widely available polysaccharides in nature, with low toxicity, high biodegradability, and easy chemical modification. Aldehyde-containing dextran reacts easily with amine compounds, and the aldehydes form Schiff bases. This reaction

[a]*Program in Biotechnology, Faculty of Science, Chulalongkorn University, Bangkok, Thailand*
[b]*School of Materials Science, Japan Advanced Institute of Science and Technology, Ishikawa, Japan*
[c]*Faculty of Engineering Department of Environmental Applied Chemistry, University of Toyama, Toyama, Japan*
E-mail: mkazuaki@jaist.ac.jp
Electronic Supplementary Information (ESI) available: [details of any supplementary information available should be included here]. See DOI: 10.1039/x0xx00000x

is used to develop bioadhesives[29,30], drug delivery carriers[27], and cell scaffolds[31]. We discovered, by using 2-D nuclear magnetic resonance imaging, that Schiff base formation leading to chemical cross-linking also triggered the main chain degradation of dextran via a Maillard reaction[26]. In the present study, we hypothesised that biodegradability can be increased in cellulose, which has the same repeating glucose unit as dextran, through reactions involving amine compounds in the human body, and aimed to create degradable cell scaffolds. We characterised oxidised cellulose scaffolds and investigated their biodegradability under physiological conditions, their cytocompatibility, and their *in vivo* tissue compatibility for tissue engineering applications. This is the first study to produce these types of cellulose scaffolds showing amine compound-reactive degradation in the human body. This unique molecular design may be useful for producing naturally derived stimuli-responsive biodegradable biomaterials.

EXPERIMENTAL SECTION

Materials

Cellulose microcrystalline powder (20 μm) was purchased from Sigma Aldrich (St. Louis, MO, USA). Sodium periodate, di-sodium hydrogen phosphate, sodium di-hydrogen phosphate, glycine, starch soluble, 1-butyl-3-metylimidazolium chloride (BMIMCl), and all other chemical reagents were obtained from Nacalai Tesque, Inc. (Kyoto, Japan).

Scaffold fabrication

Cellulose (0.323 g) was dissolved in BMIMCl (2.15 g) by heating at 100°C for 24 h and then adding 30-60 wt % of sodium chloride with particle sizes 52–450 μm as a porogen. The resulting cellulose paste was cooled to 25°C and then sandwiched between silicon moulds (diameter: 10 mm, thickness: 3 mm). The paste was kept at room temperature for 7 d to form a gel-like material. The BMIMCl and NaCl crystals were removed by washing with distilled water and freeze-dried to form a porous scaffold. The surface of the cellulose scaffold was characterised by coating with palladium particles using a sputter coater and observed using scanning electron microscopy (SEM) (S4100, Hitachi High-Tech Corp., Tokyo, Japan). Porosity was estimated from the density of the cellulose scaffolds ($\rho_{cellilose\ scaffold}$) by assuming 1460 kg m^{-3} as the density of cellulose ($\rho_{cellilose}$), using the formula[32,33]

$$\text{porosity} = 1 - \frac{\rho_{celulose\ scaffold}}{\rho_{cellulose}}$$

The density of the scaffold was calculated by measuring its weight and dividing it by its volume. Mean pore size was determined using the average of 25 pores analysed by ImageJ software (National Institutes of Health, Bethesda, MD, USA).

Oxidation of cellulose scaffold

The obtained porous cellulose scaffolds were immersed in 10 mL of distilled water with various amounts of sodium periodate (0–2.5 g) at 50°C. The reaction proceeded at 50°C for 1 h with gentle stirring. The oxidised cellulose scaffold was washed with distilled water three times and then freeze-dried.

Determination of aldehyde introduction to cellulose

The aldehydes introduced to oxidised cellulose were evaluated by simple iodimetry[24]. One hundred milligrams of oxidised cellulose was added to an I_2 solution (20 mL, 0.05 mol/L), followed by addition of NaOH (20 mL, 1 mol/L). The oxidation reaction proceeded for 15 min. After adding H_2SO_4 (15 mL, 6.25 v/v%), the I_2 consumption was measured by titration with 0.1 mol/L $Na_2S_2O_3$ using a drop of aqueous 20 w/w% starch solution as an indicator. One mole of aldehyde group reacts with one mole of I_2 under alkaline conditions, leading to the formation of carboxylic acid, and one mole of I_2 reacts with two moles of $S_2O_3^{2-}$ ions. For each titration, readings were recorded in triplicate. The aldehyde amount introduced per gram of cellulose was calculated, and the values were converted to percent aldehyde introduced per glucose repeating unit. Upon the oxidation of all the glucose units, two aldehydes would have been introduced per unit. Therefore, the maximum % aldehyde introduced is 200 %.

Degradation of oxidised cellulose scaffold *in vitro*

Degradation of the oxidised cellulose scaffold was examined with respect to weight loss. Weight loss of the initially weighed oxidised cellulose scaffold (W_0) was monitored as a function of incubation time in both 5% glycine solution and cell culture medium (Dulbecco's modified Eagle's medium) (DMEM; Sigma Aldrich) containing 10% foetal bovine serum (FBS) at room temperature. At specified time intervals, oxidised cellulose scaffolds were removed from either the 5% glycine solution or DMEM and then dried and weighed (W_t). The weight loss ratio was defined as 100% × (W_0 - W_t)/W_0. In addition, the morphology of the remaining scaffold after degradation was investigated by SEM. The functional groups in the products were confirmed using a FT/IR-4200 spectrophotometer (JASCO, Tokyo Japan) in 4000–400 cm^{-1}. Before and after 16 h immersion in 5 % glycine solution, oxidised cellulose samples were washed using water and air-dried, and then measured directly using an attenuated total reflection (ATR) accessory.

Protein adsorption

Protein adsorption was performed by incubating the oxidised cellulose scaffolds with a 250-μm mean pore size in DMEM containing 10% FBS. Oxidised cellulose scaffolds of 1.0 cm in diameter and 0.3 cm in thickness, without cells, were incubated for 1 d in DMEM. The scaffolds were washed three times with phosphate-buffered saline (PBS) and then incubated with 0.1 mL sodium dodecyl sulphate solution for 1 h at 37°C. The amount of protein adsorbed was calculated from the concentration of protein in the supernatant using a commercial bicinchoninic acid (BCA) protein assay kit (Thermo Scientific, Waltham, MA, USA) with bovine serum albumin as a standard. In the BCA assay, peptides containing three or more amino acid residues form a purple-coloured chelate complex with cupric ions (Cu^{2+}) in an alkaline environment containing sodium potassium tartrate.

Cell growth investigation

We investigated cell proliferation on oxidised cellulose scaffolds with a mean pore size of 250 μm to evaluate the effect of the oxidation degree on cell growth. Before culturing the cells on the scaffolds, the scaffolds were sterilised by soaking in 70% ethanol; the ethanol solution was removed by washing the scaffolds three times with sterilised distilled water and then drying. The scaffolds were placed in a 12-well plate, and 2-mL human bone marrow mesenchymal stem cell (MSCs)[34] suspension (2.5 × 10^5 cells/mL) was added to the wells containing the scaffolds. Cells were cultured with the oxidised cellulose scaffolds for 3, 5, or 7 days in a CO_2 incubator, without stirring, at 37°C. Cell numbers were counted using the CCK-8 kit (Dojindo Molecular Technologies, Kumamoto, Japan). MSCs were cultured in accordance with the regulations of the Life Science Committee of Japan Advanced Institute of Science and Technology.

Morphology of cells on oxidised cellulose scaffolds

MSCs (2.5×10^5 cells/scaffold) were seeded onto oxidised cellulose scaffolds and analysed by SEM after 2 weeks of culture to observe the morphology of cells on the scaffolds. The oxidised cellulose scaffolds with cells were dried by blotting with absorbent papers and then washed with PBS (pH 7.4). Cells were fixed with glutaraldehyde (4% v/v in PBS) for 24 h at room temperature. The glutaraldehyde was discarded, and oxidised cellulose scaffolds with cells were washed with PBS. The oxidised cellulose scaffolds with cells were subjected to dehydration in sequential dehydration in graded ethanol (60%, 70%, 80%, 90%, and 100%). The scaffolds were removed, dried, and stored at 4°C until imaging. The scaffolds with cells were coated with palladium prior to SEM observation.

Animal implantation

Oxidised cellulose scaffolds were implanted under the skin of the flanks of rats (Sprague-Dawley rats, 9 weeks of age, male) under sterile conditions in a clean room. All experiments were performed according to the guidelines of the Animal Welfare Committee of the University of Toyama. The oxidised cellulose scaffolds were sterilised by soaking in 70% (v/v) ethanol for 15 min and washing with PBS (pH 7.4) three times for 10 min. Before implantation, the hair was removed by shaving. All rats were anaesthetised with 2% isoflurane. All oxidised cellulose scaffolds (diameter: 10 mm, thickness: 3 mm) were subcutaneously implanted (N=6 rats; one implant per rat). The body weights of the rats were regularly measured until 1 month after implantation. The rats were sacrificed after either 1 week, 1 month, or 3 months. At harvest, the implantation sites were cut in a manner that retained the full thickness of the implantation site.

Histological analysis

Specimens were fixed with 4% *p*-formaldehyde solution overnight and immersed in 30% sucrose in PBS for 2–4 d. They were then dehydrated by sequential dehydration in graded ethanol (70%, 80%, and 90%) for 1 h. After immersion in 100% ethanol for 20 min, the samples were submerged in a xylene-ethanol mixture of a 3:1 ratio of xylene-to-ethanol for 30 min, 100% xylene for 3 min (twice), 1:1 xylene-to-paraffin mixture at 65–75 °C for 30 min, and 100% paraffin for 30 min (three times). Next, the specimens were immersed in paraffin solution at 65°C and cooled in an ice bath to solidify the paraffin containing the tissue samples.

Paraffin sections (thickness: 10 μm) were prepared using a microtome (RM2235, Leica Biosystems, Wetzlar, Germany) and affixed to glass slides. These glass slides were immersed two times for 3 min in xylene to remove the paraffin. Next, the slides were immersed in ethanol twice for 2 min each, 90% ethanol for 2 min, 80% ethanol for 2 min, and 70% ethanol for 2 min. Finally, the samples were immersed in water for 30 min and dried overnight at room temperature.

Tissue sections on the slides were treated with blocking reagent (20% Blocking One (Nacalai Tesque) in PBS) for 2 h. Next, a blocking solution containing anti-monocyte/macrophage antibodies (1:100; mouse monoclonal (ED1) IgG_1, Millipore, Temecula, CA, USA) was incubated with the tissue sections for 2 h. After washing with PBS, tissue sections were stained with anti-mouse IgG_1-Alexa 594 antibody (Thermo Fisher Scientific) and Hoechst33258 (Dojindo) for 30 min; these samples were then washed with PBS. The localisation of secondary antibody was analysed with a fluorescence microscope (IX70, Olympus Optical Co. Ltd., Tokyo, Japan).

RESULTS AND DISCUSSION

Cellulose scaffold characterisation

When the 15 w/w% cellulose BMIMCl solution was heated to 100°C for 24 h, a transparent homogenous material with high viscosity was obtained. For scaffold formation, the homogenous cellulose mixture was kept at room temperature for 1 week. The excess ionic liquid leached out was removed from the material for 7 d during the scaffold formation process. The cellulose scaffold was purified by washing with distilled water to remove excess ionic liquid. **Figure 1** shows the cellulose scaffold without NaCl crystals as a porogen before and after leaching with distilled water. Before leaching, the cellulose scaffold was transparent and hard (**Figure 1A**), whereas after leaching, it became turbid and firm in shape (**Figure 1B**).

When NaCl crystals were incorporated into the cellulose BMIMCl solution, porous scaffolds were obtained after the

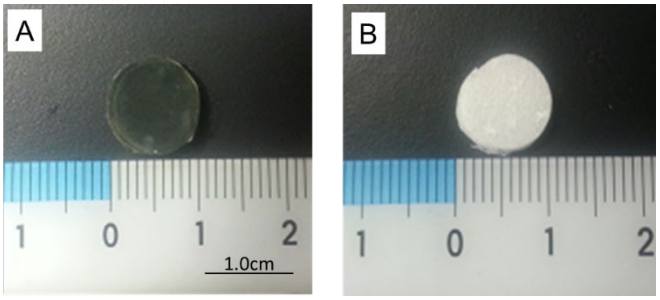

Figure 1. Photographs of cellulose scaffolds (A) before leaching and (B) after leaching.

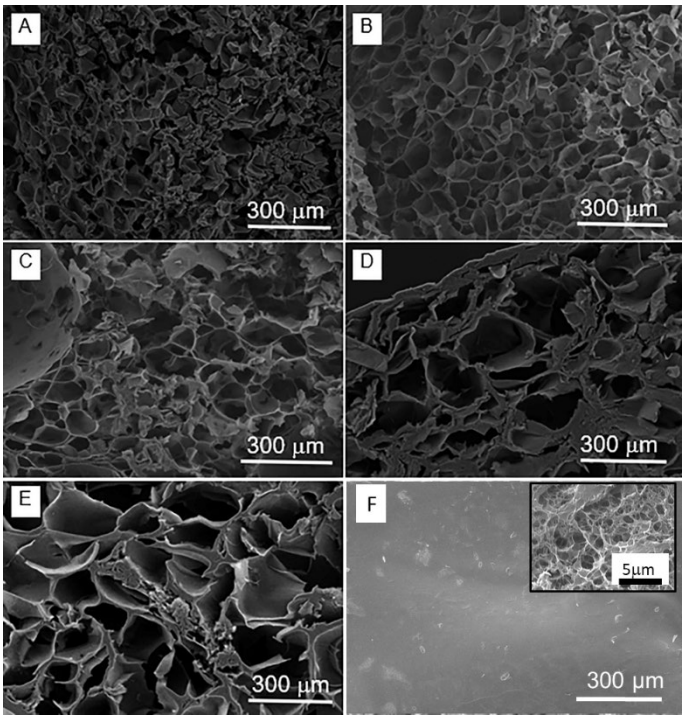

Figure 2. SEM photographs of the cellulose scaffold structure after leaching. The scaffolds contained 50 wt% NaCl with different particle sizes: (A) 52 μm, (B) 75 μm, (C) 100 μm, (D) 150 μm, (E) 250 μm, and (F) without NaCl. The inset of (F) is at a higher magnification.

leaching process[35]. **Figure 2** shows SEM images of the interconnected pores in the cellulose scaffold with differences in the mean pore size, which increased after adding sodium chloride as a porogen. The pore size increased with increasing NaCl particle sizes. According to our SEM observations, the pore sizes ranged from approximately 50 to 250 μm (**Table S1**). In samples without NaCl, the pore size was less than 2 or 3 μm, suggesting that cell penetration was impossible. Moreover, the NaCl content in the cellulose scaffold varied from 30w/w% to 60w/w%, which was correlated with an NaCl mean pore size of 250 μm (**Figure S1, Table S2**). Porosity could be controlled between 60-70% (**Table S3**). It has been reported that a pore size of around 300 μm is optimal in collagen cell scaffolds, and our results were consistent with this finding,[36] as they indicated that the mean pore size in the cellulose scaffold increased as the NaCl content increased (Table S2). Therefore, the cellulose concentration decreased as the NaCl content increased. As the concentration of cellulose decreased, the scaffold cohesiveness decreased and tended to have a more porous structure. In addition, incomplete dispersion of cellulose due to the high concentration of NaCl further expanded the interconnected pore size.

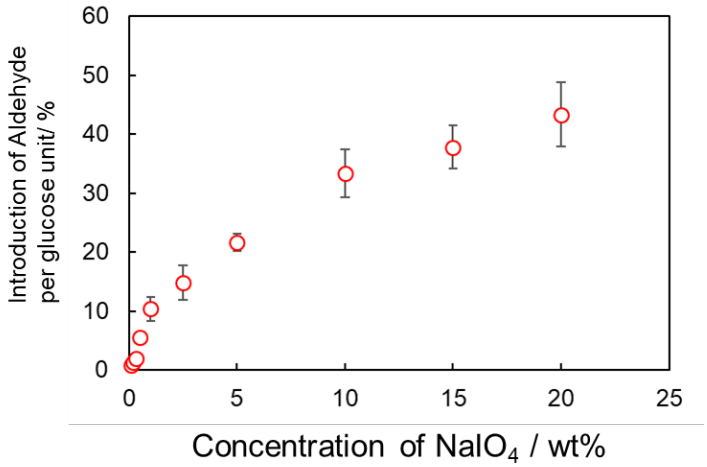

Figure 3. Introduction of aldehyde per glucose unit in cellulose by Malaprade reaction. Data represent mean ± standard deviation (N = 3).

Aldehyde introduction to oxidised cellulose scaffolds

The aldehyde content of oxidised cellulose scaffolds increased with the concentration of $NaIO_4$ at a constant time of oxidation (**Figure 3**, **Table S4**). Aldehyde introduction depends on the concentration of periodate, time, and temperature. We performed the reaction at 50°C for the fixed time; most studies using the oxidation of cellulose to yield 2,3 dialdehyde cellulose were carried out at temperatures of 55°C or below. Above 55°C, the periodate is unstable and deteriorates to liberate iodine, making it difficult to accurately determine the amount of periodate consumption. The reaction proceeds very slowly when conducted at room temperature or below 35°C. Verma and Kulkarni[37] reported that oxidising cellulose at different temperatures affects the percentage of cellulose converted to 2,3 dialdehyde cellulose, and that at 55°C, the percentage of cellulose converted to 2,3 dialdehyde cellulose is more than that converted at 35°C. Because of the loss of the crystalline structure of cellulose powder during the fabrication of cellulose scaffolds[5], the cellulose becomes more susceptible to the reaction with periodate. In this study, we denoted aldehyde-containing cellulose as X% Ald-Cel (e.g., 0% Ald-Cel, 21.7% Ald-Cel) based on the aldehyde content per glucose unit. Mean pore size and porosity showed no significant changes due to oxidation (Table S1, S3).

Degradation of oxidised cellulose scaffolds *in vitro*

The degradation of oxidised cellulose scaffolds was investigated by measuring their weight loss in 5% glycine. We used glycine to confirm that the degradation of cellulose occurred in the same manner as in the oxidised dextran case via Schiff base formation reaction between the aldehyde in the Ald-Cel and amino group in the glycine[26]. The percent weight loss of oxidised cellulose scaffolds in 5% glycine solution is shown in **Figure 4.**

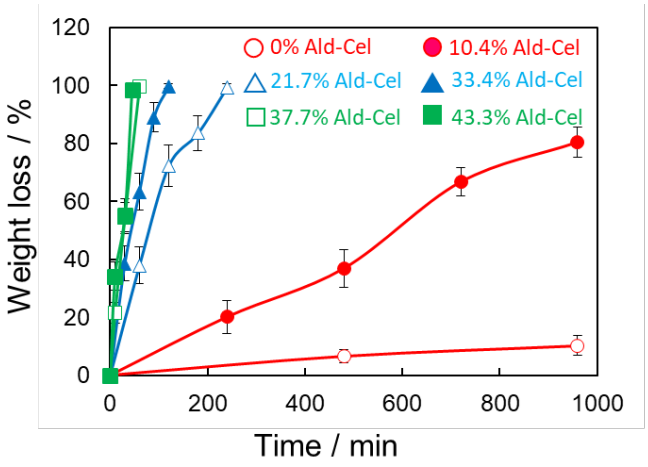

Figure 4. Oxidised cellulose scaffold degradation in 5% glycine solution over 16 h. Data represent mean ± standard deviation (N = 3).

The results indicated that the degradation rate of the oxidised cellulose scaffold depended on the degree of oxidation. Interestingly, the 43.3% Ald-Cel scaffold degraded the fastest, with complete degradation occurring after 45 min. In contrast, the 0%Ald-Cel scaffold exhibited only a slight weight loss, possibly due to the detachment of small fragments from the bulk scaffold during the degradation assay. For the 37.7%, 33.4%, and 21.7% Ald-Cel scaffolds, degradation was complete after 1, 2, and 4 h, respectively. However, the 10.4% Ald-Cel scaffold exhibited partial degradation (approximately 80%) after 16 h. In 5% glycine solution, the aldehyde content was too high to control the degradation of cell scaffolds; therefore, we measured the degradation of cellulose with less introduced aldehyde. Accordingly, the degradation times of 0%, 0.9%, 1.3%, and 1.9% Ald-Cel scaffolds in 5% glycine solution for 8 weeks were measured (**Figure S2**). After 8 weeks, 56.3%, 37.4%, and 31.9% degradation was observed in the 1.9%, 1.3%, and 0.9% Ald-Cel scaffolds, respectively. The degradation rate increased almost linearly, suggesting that the cellulose scaffolds were uniformly oxidised by the introduced aldehyde, and not only on the surface. However, when using scaffolds for cell culture and tissue engineering, they must be degraded under physiological conditions. Therefore, we checked the degradability in culture

medium, which mimics the human body fluid containing amino acids and proteins.

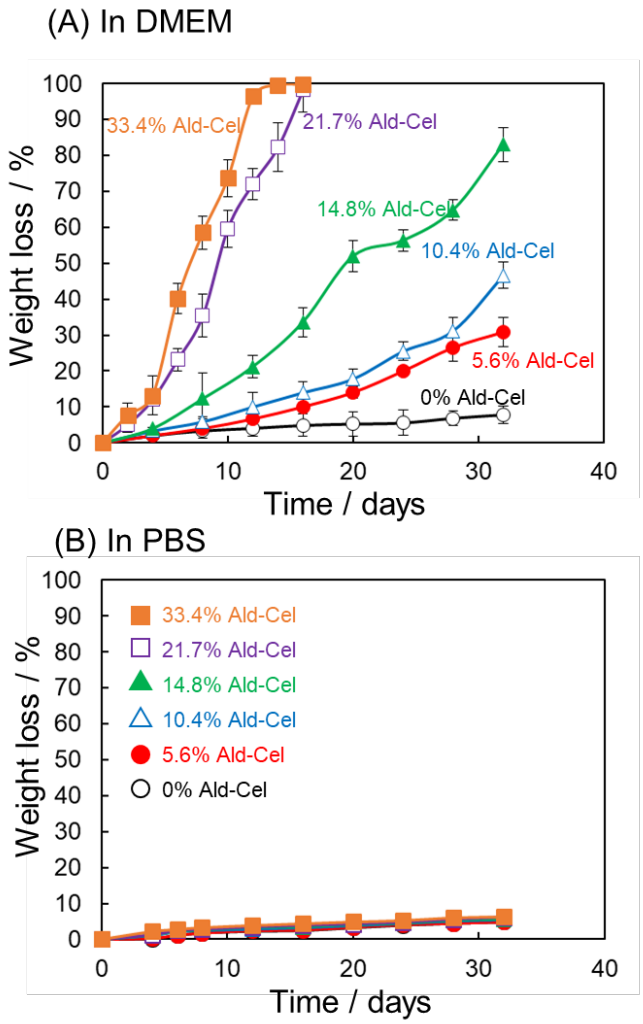

Figure 5. Ald-Cel scaffold degradation in (A) culture media and (B) PBS at 37°C over 32 d. Data represent mean ± standard deviation (N = 3).

When 0–33.4% Ald-Cel scaffolds were immersed in DMEM with 10% FBS at 37°C in a CO_2 incubator without stirring for 8 weeks, the 21.7% and 33.4% Ald-Cel scaffolds degraded the fastest, being fully degraded after about 15 days. The 0%, 5.6%, 10.4%, and 14.8% Ald-Cel scaffolds were partially degraded, with 7.8%, 32.1%, 48.9%, and 83.0% weight loss after 32 days, respectively (**Figure 5A**). Importantly, all Ald-Cel scaffolds had low degradation ratios after immersion in PBS for 32 days (**Figure 5B**). Further, we used FTIR for the measurement of various aldehyde containing cellulose before and after immersion in glycine solution (Figure 6). Figure 6A showed that even 10.4% Ald-Cel did not show a peak at around 1730 cm^{-1}, a characteristic peak of carbonyl stretching from aldehyde groups, due to the formation of hemiacetals[38]. After immersion in glycine solution, especially in 10.4%Ald-Cel, the band at 1650 cm^{-1} indicating a Schiff base formation, was detected. In the Maillard reaction pathway after Schiff base formation, secondary amines could be obtained via Amadori rearrangement (N-H stretching 3200cm^{-1}, N-H bending 1600 cm^{-1}, C-N stretching 1110-1120 cm^{-1}). Furthermore, CH_2 containing Maillard reaction products (osone, etc.) can be detected at 1510 and 1410cm^{-1} (C-H bending)[26,39,40]. In a previous study, oxidised dextran did not degrade in PBS because Malaprade oxidation itself was unable to degrade the dextran chain[26]. These results strongly indicate that scaffold degradation is triggered by a Schiff base formation reaction and occurs through a Maillard reaction, similar to the observations of a previous study on oxidised dextran[26]. This is consistent with the results of the 0.9 and 1.9% Ald-Cel scaffolds in 5% glycine, in which less Maillard reaction products could be found using FTIR but showed less degradation in the present study (Figure S2).

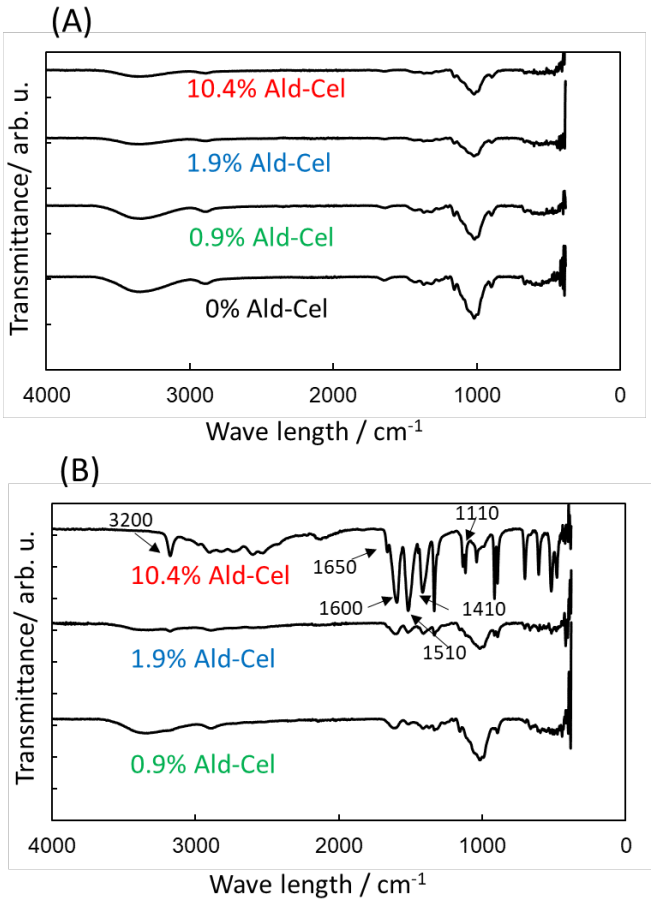

Figure 6. FTIR spectra of Ald-Cel scaffolds (A) before and (B) after immersion in 5 % glycine for 16 h.

There have been many reports of the biodegradability of oxidised cellulose; for example, some studies used tris(hydroxymethyl)aminomethane buffer (containing an amino group) for the degradation assay[41]. In such a case, degradation may be initiated through the reaction between the aldehyde and amine in the buffer solution. It was also reported that highly oxidised cellulose can be water-soluble in hot water[42]. This finding applies to aqueous nanomaterials; however, our ability to control degradability in PBS was minimal, and degradation began as soon as the Ald-Cels were immersed in the amine-containing solution. The Ald-Cels are stimuli-responsive degradable scaffolds and can be degraded in response to protein molecules in the human body.

In addition, 0% and 5.6% Ald-Cel scaffolds with a mean pore size of 250 μm were immersed in DMEM to investigate the

scaffold morphology degradation after 1 and 2 weeks. The SEM images illustrate the time-dependent morphological changes in both 0% and 5.6% Ald-Cel scaffolds (**Figure 6**). After both 1 and 2 weeks, the 0%Ald-Cel scaffold morphology showed no significant changes (**Figure 7A**, **7B**); however, significant morphological changes in 5.6% Ald-Cel scaffolds were observed after 2 weeks (**Figure 7C**, **7D**), as the destruction of the internal scaffold structure changed the surface morphology. Ideally, a scaffold would become completely degraded and replaced with regenerated extra cellular matrix, eliminating the need for surgical removal of the scaffold, although the scaffold should be degraded at a controlled rate. Sung et al. studied the effect of the degradation rate on cell viability and cell migration[43], and showed that rapid degradation negatively affects cell viability and cell migration both *in vitro* and *in vivo*.

We found that the degradation of Ald-Cel scaffolds depends on the degree of oxidation. The results suggest that the Ald-Cel scaffold degradation rate was affected by the concentration of aldehyde groups and accelerated scaffold degradation compared to non-oxidised cellulose scaffolds. In addition, we studied the degradation of Ald-Cel scaffolds in DMEM to mimic the conditions of fluids in the human body. The results aligned with the degradation behaviour in 5% glycine. Interestingly, the degradation rate in DMEM was slower than that in 5% glycine because the amino group content in 5% glycine is much higher than that in DMEM.

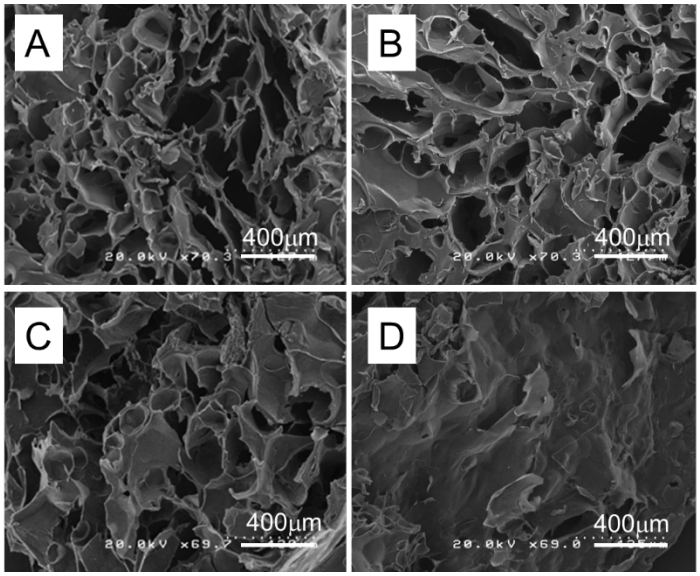

Figure 7. SEM micrographs of Ald-Cel scaffold degradation in DMEM. (A) 0%Ald-Cel scaffold after 1 week, (B) 0%Ald-Cel scaffold after 2 weeks, (C) 5.6%Ald-Cel scaffold after 1 week, and (D) 5.6%Ald-Cel scaffold after 2 weeks. All Ald-Cel scaffolds had a mean pore size of approximately 250 μm.

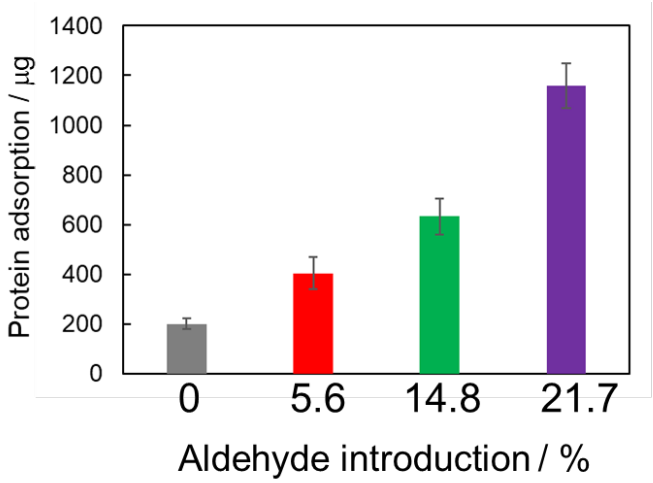

Figure 8. Protein adsorption to 0%, 5.6%, 14.8%, and 21.7% Ald-Cel scaffolds with 250-μm mean pore sizes. Data represent mean ± standard deviation (N=3).

Protein adsorption

The interaction between cells and proteins is directly related to cell differentiation, growth, adhesion, migration, and apoptosis. Adsorption of proteins to the scaffolds was evaluated to understand cell behaviour on scaffolds. **Figure 8** shows the protein adsorption of 0%, 5.6%, 14.8%, and 21.7% Ald-Cel scaffolds with a mean pore size of 250 μm. The 21.7%Ald-Cel scaffold had the highest level of protein adsorption (1.16×10^3 μg/scaffold). This indicates that protein adsorption increased in response to the increase in oxidation degree. Because of the Malaprade reaction, which results in a large amount of aldehyde groups, the amine groups react with the aldehyde groups via a Schiff base reaction. In contrast, the hydroxyl group in the glucopyranose ring cannot react with the amine groups, and therefore may not induce protein interaction.

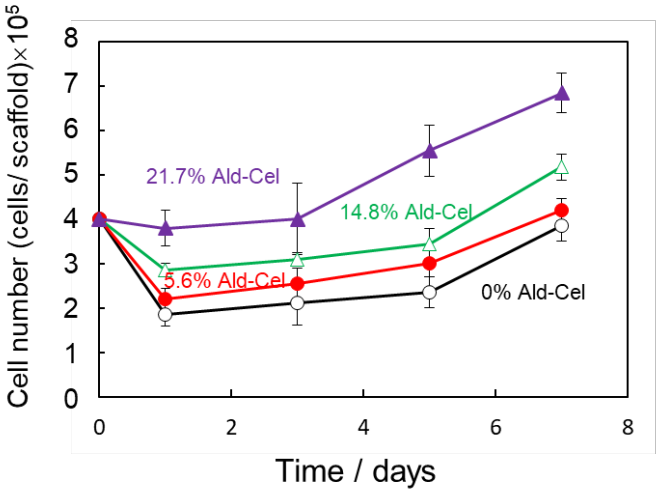

Figure 9. Effect on cell growth, of the oxidation degree of cellulose scaffolds with a mean pore size of 250 μm. Data represent mean ± standard deviation (N=3).

Effect of oxidation degree on cell growth

MSCs were cultured with 0%, 5.6%, 14.8%, and 21.7% Ald-Cel scaffolds for 1, 3, 5, and 7 days (**Figure 9**). The 21.7%Ald-Cel scaffolds showed the highest cell numbers, with approximately 6.65×10^5 cells/scaffold at the day 7. At the same day, the 0%, 5.6%, and 14.8% Ald-Cel scaffolds had 3.95×10^5, 4.13×10^5, and 5.20×10^5 cells/scaffold, respectively. These results indicate that on the first day, many cells could not attach to the scaffolds with lower oxidation rates, leading to slow proliferation. This

agrees with the results of a prior study suggesting that native cellulose promotes low levels of cell growth[44]. In contrast, 21.7%Ald-Cel exhibited significant cell adhesion after 1 d of culturing. Thus, the cell numbers may have increased as the degree of oxidation in the scaffolds increased.

The reaction of cells with aldehyde-containing scaffolds may have two effects. Because of the increased protein adsorption to oxidised cellulose, cells attach to the surface via adsorbed cellular adhesive proteins such as laminin and fibronectin[45]. In fact, before cells adhere, adsorption of cellular adhesive proteins to the polymer surface occurs. Subsequently, cells with attached proteins adhere to the polymer surface. Hence, cell growth is correlated with protein adsorption. The results of our study indicated that cellular adhesive proteins attached to the oxidised cellulose without denaturing and maintained their properties. Another possibility, according to a previous report[46], is that cells attach to the surface via a reaction between aldehydes and cell surface proteins. However, damage to the cells caused by the reaction would be negligible compared to that in the proliferation results.

The biocompatibility of 0% and 21.7% Ald-Cel scaffolds was also examined. SEM photographs of MSCs cultured on the 0%Ald-Cel (**Figure 10A**) and 21.7%Ald-Cel (**Figure 10B**) after 2-week culture show that cells adhered more densely to the surfaces of 21.7%Ald-Cel scaffolds, indicating that the oxidised cellulose scaffold promoted MSC growth. Generally, aldehyde groups have high cytotoxicity because of their high reactivity. However, in the previous study, polysaccharide aldehydes did not exhibit such high toxicity because most aldehyde groups adopted the hemiacetal structure for stabilization[23]. This may explain the high cytocompatibility of the Ald-Cels.

Animal testing

The Ald-Cel scaffolds were subcutaneously implanted into the backs of rats. The rats were sacrificed after 1 week, 1 month, or 3 months. We measured the changes in the rats' body weights until 1 month after the day of surgery (**Figure S3**). We observed nearly the same weight increase in all groups, suggesting that no specific damage occurred from the oxidation of cellulose. **Figure 11** shows haematoxylin and eosin (H&E) staining of the tissue sections. **Figures 11A–C** illustrate the interaction between 0%Ald-Cel scaffolds and host tissue. After 1 week, the morphology of scaffolds was not clearly visible because of high levels of inflammation and bleeding following surgery. For the 0%Ald-Cel scaffolds after 1 and 3 months (**Figures 11B, C**), the scaffold structure was maintained. Cellular infiltration of the scaffold **(Figure 11B**) was not observed after 1 month; after 3 months, cells partially infiltrated the scaffold. The cells had accumulated around the outside and near the edge of the scaffold. Inflammation of the host tissue was not clearly visible because it had been encapsulated by fibrous tissue, a normal host response to non-degradable materials after 3 months[47] (**Figure 11C**).

In the case of the 5.6% Ald-Cel scaffolds after 1 and 3 months (**Figure 11E, 11F)**, the cells moderately infiltrated the scaffold, and a few cells spread around the scaffold. However, degradation of the scaffold did not occur, despite initial inflammation (**Figure 11E**). The 5.6%Ald-Cel scaffolds, after 3 months, exhibited a large number of infiltrated cells. Meanwhile, inflammation persisted for 3 months (**Figure 11F**).

Interestingly, the 14.8%Ald-Cel scaffolds exhibited high levels of degradation with low levels of inflammation after 1 and 3 months (**Figure 11H, I**). After 1 month, nearly all cells had infiltrated the scaffolds with high levels of degradation, although the scaffolds caused less inflammation in the host tissue (**Figure 11H**). Subsequently, the 14.8%Ald-Cel scaffolds were nearly fully degraded after 3 months, although the inner structure of the scaffold remained intact (black arrow in **Figure**

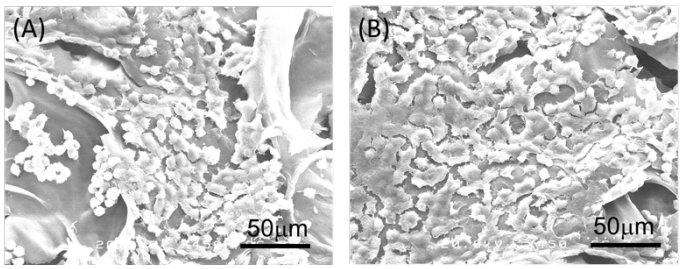

Figure 10. SEM micrographs showing MSC growth on the (A) 0%Ald-Cel and (B) 21.7%Ald-Cel scaffold after 2 weeks.

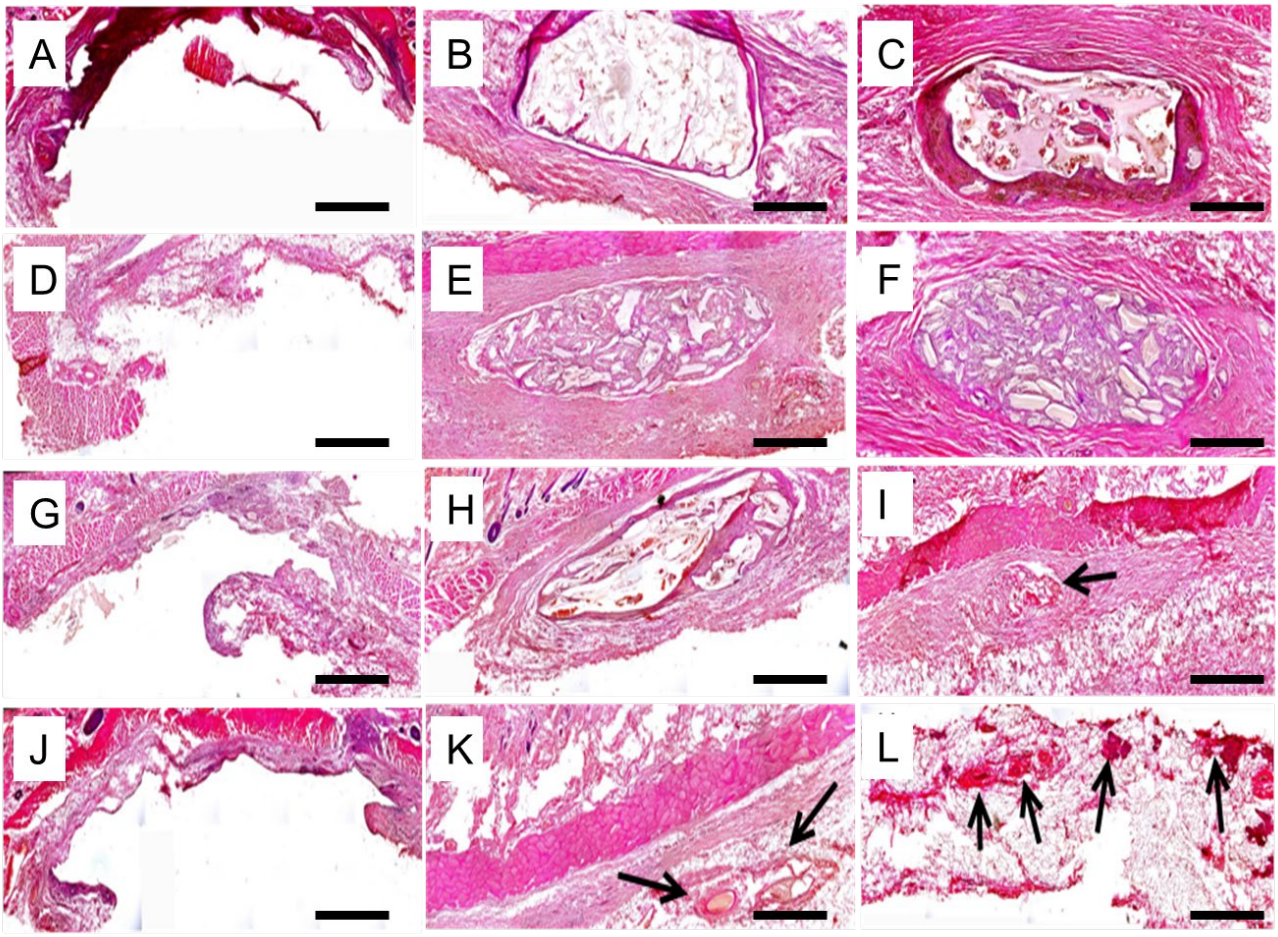

Figure 11. H&E staining was performed to investigate the real-time interaction between oxidised cellulose scaffolds and the host. The images show 0%Ald-Cel scaffolds after (A) 1 week, (B) 1 month, and (C) 3 months; 5.6%Ald-Cel scaffolds after (D) 1 week, (E) 1 month, and (F) 3 months; 14.8%Ald-Cel scaffolds after (G) 1 week, (H) 1 month, and (I) 3 months; and 21.7%Ald-Cel scaffolds after (J) 1 week, (K) 1 month, and (L) 3 months. Scale bars: 500 μm.

11I). Moreover, the host tissue at the centre of the scaffold and adjacent area became plenary compared with host tissue without implantation (**Figure 11I**).

The degradation of the 21.7% Ald-Cel scaffolds after 1 month was more pronounced than that of the 5.6% and 14.8% Ald-Cel scaffolds, leaving few remaining scaffold structures. After 1 month, the scaffolds became lean and small (black arrow in **Figure 11K**). A large number of cells spread within the scaffold (**Figure 11K**). However, the host tissue exhibited high levels of inflammation that persisted throughout the 3-month observation period. After 3 months, the 21.7% Ald-Cel scaffolds became tattered and divided into three specimens (black arrow in **Figure 11L**), suggesting that the scaffold had undergone intense degradation. The high level of inflammation in the host tissue was attributed to the high degree of oxidation of the scaffold. Generally, aldehyde groups have high toxicity, because of their high reactivity, and cause severe inflammation[48]. However, aldehydes in polysaccharides can form a hemiacetal structure with neighbouring hydroxyl groups to reduce reactivity and toxicity. Although oxidised cellulose has pro-inflammatory activity, this only applies to its wound healing and anti-haemorrhage properties[49,50].

Moreover, inflammation caused by Ald-Cel scaffold implantation was observed by performing immuno-staining of macrophages (**Figure 12**). At 1 week after implantation, the 14.8% and 21.7% Ald-Cel scaffolds exhibited high levels of inflammation (red spots) surrounding the outside of the scaffolds (white dashed line) (**Figures 12G, J**) because only 1 week had passed since the operation. At 1 month after implantation, the 5.6% Ald-Cel scaffold caused significant inflammation in the host tissue that had infiltrated the scaffold (**Figure 12E**). After 3 months, inflammation remained in all Ald-Cel scaffolds (**Figure 12C, F, I, L**). Interestingly, the 14.8%Ald-Cel scaffolds showed the lowest level of inflammation after 3 months (**Figure 12I**). This result was further supported by and correlated with the results of H&E staining. It was reported that Maillard reaction products derived from sugars and amino acids exhibit antioxidant and anti-inflammatory activities[51]. The anti-inflammatory activities of the Maillard reaction products and pro-inflammatory activity of the aldehydes may counteract each other in the optimal formulation of oxidised cellulose.

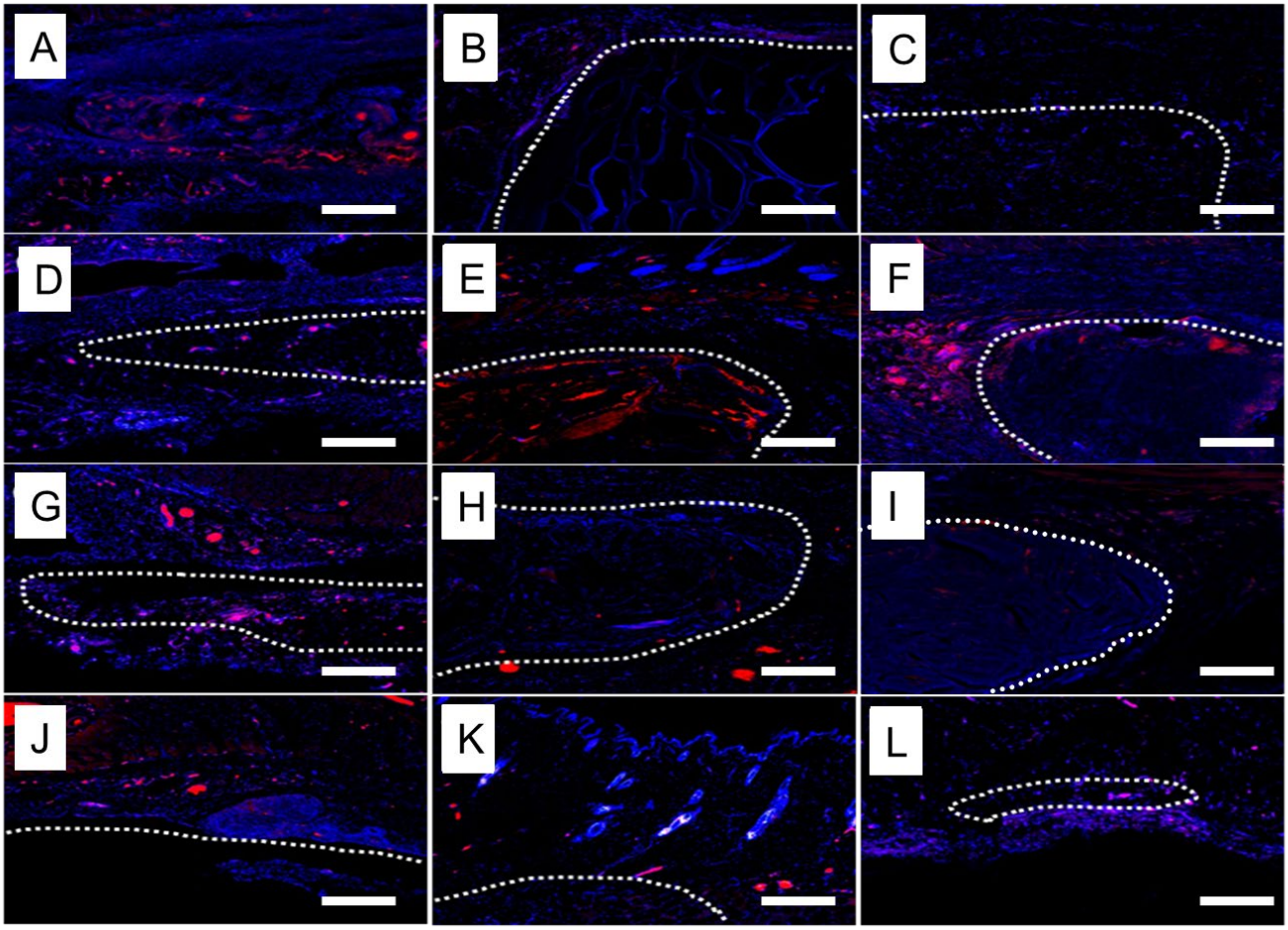

Figure 12. Hoechst33258 and anti-monocyte/macrophage antibody staining was performed to investigate inflammation during implantation. The images show 0%Ald-Cel scaffolds after (A) 1 week, (B) 1 month, and (C) 3 months; 5.6%Ald-Cel scaffolds after (D) 1 week, (E) 1 month, and (F) 3 months; 14.8%Ald-Cel scaffolds after (G) 1 week, (H) 1 month, and (I) 3 months, and 21.7%Ald-Cel scaffolds after (J) 1 week, (K) 1 month, and (L) 3 months. Scale bars: 500 μm.

These *in vivo* results indicate that the biocompatibility of oxidised cellulose depends significantly on the aldehyde content. Cytocompatibility was higher with higher aldehyde content because of protein adhesion. However, faster degradation through the Maillard reaction may have induced inflammation when the aldehyde content was higher. It was likely that the degradation products stimulated the macrophages. These results suggest that 14.8% Ald-Cel is an appropriate oxidised cellulose with suitable levels of biodegradability, cytocompatibility, and *in vivo* tissue compatibility. Therefore, although the oxidation ratio of cellulose was optimised, Ald-Cel scaffolds may be useful in tissue engineering applications because of their biocompatibility, cell adhesion, and controllable biodegradability. Studies focused on bone tissue engineering using oxidised cellulose are currently ongoing in our group, and the results will be presented in due course.

CONCLUSION

In this study, we observed that the degradability of oxidised cellulose in the presence of amine compounds depended on the aldehyde introduction ratio. Oxidised cellulose had good protein adhesion and cell growth on its surface. *In vivo* tissue reactions showed high levels of inflammation caused by oxidised cellulose because of fast degradation, but inflammation was controlled by the aldehyde content. Optimal aldehyde contents (14.8% Ald-Cel) produced low levels of inflammation and moderate levels of degradation *in vivo*. Although further studies such as nuclear magnetic resonance or molecular weight analysis of cellulose materials are needed to understand degradation at the molecular level, this study demonstrated that the biodegradability of cellulose could be controlled by oxidation and that biodegradable scaffolds introduced under certain physiological conditions can be useful as tissue engineering materials.

Conflicts of interest

There are no conflicts of interest to declare.

Corresponding Author
Kazuaki Matsumura
Email: mkazuaki@jaist.ac.jp

REFERENCES

1 S. Martino, F. D'Angelo, I. Armentano, J. M. Kenny and A. Orlacchio, *Biotechnol. Adv.*, 2012, 30, 338–351.
2 Y. Ikada, *J. R. Soc. Interface*, 2006, 3, 589–601.

3 Y. Brechet, D. Bassetti, D. Landru and L. Salvo, *Prog. Mater. Sci.*, 2001, 46, 407–428.
4 F. J. O'Brien, *Mater. Today*, 2011, 14, 88–95.
5 E. J. Shin, S. M. Choi, D. Singh, S. M. Zo, Y. H. Lee, J. H. Kim and S. S. Han, *Cellulose*, 2014, **21**, 3515–3525.
6 J. M. Moran, D. Pazzano and L. J. Bonassar, *Tissue Eng.*, 2003, **9**, 63–70.
7 M. Santoro, S. R. Shah, J. L. Walker and A. G. Mikos, *Adv. Drug Deliv. Rev.*, 2016, 107, 206–212.
8 M. Patel, T. Nakaji-Hirabayashi and K. Matsumura, *J. Biomed. Mater. Res. Part A*, 2019, **107**, 1094–1106.
9 S. Van Vlierberghe, P. Dubruel and E. Schacht, *Biomacromolecules*, 2011, 12, 1387–1408.
10 S. Liu, J. Zeng, D. Tao and L. Zhang, *Cellulose*, 2010, **17**, 1159–1169.
11 S. Liu, D. Tao and L. Zhang, *Powder Technol.*, 2012, **217**, 502–509.
12 H. P. S. Abdul Khalil, A. H. Bhat and A. F. Ireana Yusra, *Carbohydr. Polym.*, 2012, 87, 963–979.
13 C. Chen, T. Zhang, Q. Zhang, Z. Feng, C. Zhu, Y. Yu, K. Li, M. Zhao, J. Yang, J. Liu and D. Sun, *ACS Appl. Mater. Interfaces*, 2015, **7**, 28244–28253.
14 Q. Chen, R. P. Garcia, J. Munoz, U. Pérez De Larraya, N. Garmendia, Q. Yao and A. R. Boccaccini, *ACS Appl. Mater. Interfaces*, 2015, **7**, 24715–24725.
15 S. Coseri, G. Biliuta, B. C. Simionescu, K. Stana-Kleinschek, V. Ribitsch and V. Harabagiu, in *Carbohydrate Polymers*, Elsevier, 2013, vol. 93, pp. 207–215.
16 P. A. Larsson, T. Pettersson and L. Wågberg, *Green Mater.*, 2014, **2**, 163–168.
17 YACKEL and EC, *J Am Chem Soc*, 1942, **64**, 121–127.
18 N. R. Kunio and M. A. Schreiber, in *Consultative Hemostasis and Thrombosis: Third Edition*, Elsevier Inc., 2013, pp. 538–545.
19 A. Isogai, T. Saito and H. Fukuzumi, *Nanoscale*, 2011, 3, 71–85.
20 X. Mo, H. Iwata, S. Matsuda and Y. Ikada, *J. Biomater. Sci. Polym. Ed.*, 2000, **11**, 341–351.
21 S. F. Plappert, S. Quraishi, N. Pircher, K. S. Mikkonen, S. Veigel, K. M. Klinger, A. Potthast, T. Rosenau and F. W. Liebner, *Biomacromolecules*, 2018, **19**, 2969–2978.
22 U. J. Kim, S. Kuga, M. Wada, T. Okano and T. Kondo, *Biomacromolecules*, 2000, **1**, 488–492.
23 K. Pietrucha, E. Marzec and M. Kudzin, *Int. J. Biol. Macromol.*, 2016, **92**, 1298–1306.
24 S. H. Hyon, N. Nakajima, H. Sugai and K. Matsumura, *J. Biomed. Mater. Res. - Part A*, 2014, **102**, 2511–2520.
25 K. Matsumura, N. Nakajima, H. Sugai and S. H. Hyon, *Carbohydr. Polym.*, 2014, **113**, 32–38.
26 W. Chimpibul, T. Nagashima, F. Hayashi, N. Nakajima, S. H. Hyon and K. Matsumura, *J. Polym. Sci. Part A Polym. Chem.*, 2016, **54**, 2254–2260.
27 P. Nonsuwan and K. Matsumura, *ACS Appl. Polym. Mater.*, 2019, **1**, 286–297.
28 P. Nonsuwan, A. Matsugami, F. Hayashi, S. H. Hyon and K. Matsumura, *Carbohydr. Polym.*, 2019, **204**, 131–141.
29 M. Araki, H. Tao, N. Nakajima, H. Sugai, T. Sato, S. H. Hyon, T. Nagayasu and T. Nakamura, *J. Thorac. Cardiovasc. Surg.*, 2007, **134**, 1241–1248.
30 M. Takaoka, T. Nakamura, H. Sugai, A. J. Bentley, N. Nakajima, N. J. Fullwood, N. Yokoi, S. H. Hyon and S. Kinoshita, *Biomaterials*, 2008, **29**, 2923–2931.
31 X. Zhao, P. Li, B. Guo and P. X. Ma, *Acta Biomater.*, 2015, **26**, 236–248.
32 C. C. Sun, *Int. J. Pharm.*, 2008, **346**, 93–101.
33 H. Sehaqui, Q. Zhou, O. Ikkala and L. A. Berglund, *Biomacromolecules*, 2011, **12**, 3638–3644.
34 S. Tsutsumi, A. Shimazu, K. Miyazaki, H. Pan, C. Koike, E. Yoshida, K. Takagishi and Y. Kato, *Biochem. Biophys. Res. Commun.*, 2001, **288**, 413–419.
35 R. Nazarov, H. J. Jin and D. L. Kaplan, *Biomacromolecules*, 2004, **5**, 718–726.
36 C. M. Murphy, M. G. Haugh and F. J. O'Brien, *Biomaterials*, 2010, **31**, 461–466.
37 A. J. Varma and M. P. Kulkarni, *Polym. Degrad. Stab.*, 2002, **77**, 25–27.
38 J. Maia, L. Ferreira, R. Carvalho, M. A. Ramos and M. H. Gil, *Polymer (Guildf).*, 2005, **46**, 9604–9614.
39 M.-M. Han, Y. Yi, H.-X. Wang and F. Huang, *Molecules*, 2017, **22**, 938.
40 J. M. Ames, in *Biochemistry of Food Proteins*, Springer US, 1992, pp. 99–153.
41 S. Laurence, R. Bareille, C. Baquey and J. C. Fricain, *J. Biomed. Mater. Res. - Part A*, 2005, **73**, 422–429.
42 U. J. Kim, M. Wada and S. Kuga, *Carbohydr. Polym.*, 2004, **56**, 7–10.
43 H. J. Sung, C. Meredith, C. Johnson and Z. S. Galis, *Biomaterials*, 2004, **25**, 5735–5742.
44 L. Bartouilh de Taillac, M. C. Porté-Durrieu, C. Labrugère, R. Bareille, J. Amédée and C. Baquey, *Compos. Sci. Technol.*, 2004, **64**, 827–837.
45 K. M. Yamada, *J. Biol. Chem.*, 1991, **266**, 12809–12.
46 J. Wu, Y. Zheng, Z. Yang, Q. Lin, K. Qiao, X. Chen and Y. Peng, *RSC Adv.*, 2014, **4**, 3998–4009.
47 K. R. Williams and A. W. Blayney, *Biomaterials*, 1987, **8**, 254–258.
48 M. B. St Clair, E. A. Gross and K. T. Morgan, *Toxicol. Pathol.*, 1990, **18**, 353–61.
49 P. Kollar, V. Závalová, J. Hošek, P. Havelka, T. Sopuch, M. Karpíšek, D. Třetinová and P. Suchý, *Int. Immunopharmacol.*, 2011, **11**, 997–1001.
50 M. G. Jeschke, G. Sandmann, T. Schubert and D. Klein, *Wound Repair Regen.*, 2005, **13**, 324–331.
51 X. M. Chen and D. D. Kitts, *J. Agric. Food Chem.*, 2011, **59**, 11294–11303.

TABLE OF CONTENTS GRAPHIC

Cellulose scaffolds, whose biodegradation can be controlled through the reaction with amine compounds in the human body, were developed for tissue engineering applications.